**Stat3 controls tubulo-interstitial communication during chronic kidney disease**

Frank Bienaimé[1,2], Mordi Muorah[1], Lucie Yammine[1], Martine Burtin[1], Clément Nguyen[1], Willian Baron[1], Serge Garbay[3], Amandine Viau[1], Mélanie Broueilh[1], Thomas Blanc[1], Dorien Peters[4], Valeria Poli[5], Dany Anglicheau[1,6], Gérard Friedlander[1,2], Marco Pontoglio[3], Morgan Gallazzini[1], Fabiola Terzi[1]

1 INSERM U1151, Université Paris Descartes, Institut Necker Enfants Malades, Department "Growth and Signaling", Hôpital Necker Enfants Malades, Paris, France

2 Service d'Explorations Fonctionnelles, Hôpital Necker Enfants Malades, Paris, France

3 INSERM U1016 - CNRS UMR 8104, Université Paris Descartes, Institut Cochin, Paris, France

4 Department of Human Genetics, Leiden University Medical Center, Leiden, Nederland

5 Department of Biotechnology and Health Sciences, Molecular Biotechnology Center, Torino University, Torino, Italy

6 Service de Néphrologie - Transplantation, Hôpital Necker Enfants Malades, Paris, France

Running title: Stat3 triggers paracrine fibrotic signaling in CKD

Abstract word count: 176

Text word count: 2990

Corresponding author: Fabiola Terzi, MD, PhD
INSERM U1151
Team: Mechanisms and Therapeutic Strategies of Chronic Kidney Disease.
Hôpital Necker Enfants Malades
Tour Lavoisier, 6ème étage
149 Rue de Sèvres
75015 Paris, France
Phone +33 1 44495245
Fax +33 1 44490290
email fabiola.terzi@inserm.fr

**ABSTRACT**

In chronic kidney disease (CKD), tubular cells are thought to be involved in the induction of interstitial fibrosis, which in turn leads to loss of renal function. The molecular mechanisms that link tubular cells to the interstitial compartment are not clear. Here, we combined an experimental model of nephron reduction, mice from different genetic backgrounds and genetically modified animals with *in silico* and *in vitro* experiments, to demonstrate that the selective activation of Stat3 in tubular cells is crucial for the development of interstitial fibrosis. Stat3 was activated exclusively in tubular cells of lesion-prone mice after nephron reduction. The specific inactivation of *Stat3* in tubular cells resulted in reduced fibroblast proliferation and matrix synthesis. As a consequence, the extent of interstitial fibrosis was significantly reduced in $Stat3^{\Delta tub}$ transgenic mice. Mechanistically, tubular Stat3 activation triggered the expression of a specific subset of paracrine profibrotic factors, including Lcn2, Pdgfb and Timp1. Together, our results provide a molecular link between tubular and interstitial cells during CKD progression and identify Stat3 as a central regulator and a promising therapeutic target.

Key words: Stat3/kidney/fibrosis/paracrine mediators/Lcn2

## INTRODUCTION

Chronic reduction of renal function, the common denominator of chronic kidney diseases (CKD), represents a worldwide health concern. Grossly, 10% of the adult population is estimated to suffer from CKD[1]. These patients display an increased risk of death and cardiovascular morbidity that is proportional to the decline of renal function[2, 3]. Moreover, due to its progressive nature, CKD may lead to end-stage renal disease (ESRD), which requires renal replacement therapy substantially altering life quality and expectancy.

Regardless of the initial insult, all CKD are thought to share a common mechanism of progression by which the overwork imposed by compensation to the remaining nephrons leads to further nephron loss[4] which leads to the development of renal lesions. The identity of the molecular networks at the origin of the initial compensatory processes and the mechanisms leading to the subsequent appearance of lesions has only been partially elucidated. Clinical studies have shown that the decline of renal function correlates more closely with the severity of interstitial fibrosis than with glomerular damage[5-7]. Recent finding indicate that the activation of renal fibroblasts by paracrine factors play a critical role in the development of renal fibrosis[8]. It is known that the overwork imposed by adaptation lead to mechanical and metabolic stresses of tubular cells, which in turn start to synthesize soluble mediators of CKD progression, i.e. cytokines and profibrotic growth factors. Similarly, leakage of albumin from the damaged glomerular barrier also leads to the damage of tubular cells with the subsequent production of profibrotic mediators. Thus, it is tempting to speculate that, by delivering fibrogenic paracrine cues to interstitial fibroblasts, tubular cell activation is a crucial step of CKD progression.

Signal transducers and activators of transcription (Stats) are versatile transcription factors that mediate the intra-cellular signaling of various molecular pathways[9]. Stat activation begins by

their recruitment to membrane receptors where they are phosphorylated, either directly by receptors with tyrosine kinase activity or indirectly by receptor-associated tyrosine kinases. This phosphorylation allows both dimerization and nuclear accumulation of the activated Stat, which binds to cognate elements on promoters of responsive genes[10]. Among the 7 known Stat genes, Stat3 displays unique features. It has the largest spectrum of potential activators including various cytokines, hormones and growth factors[11]. Contrary to the other members, Stat3 is the only one whose inactivation leads to embryonic lethality in mice[12]. Another peculiar characteristic of Stat3 is its ability to regulate gene networks that are highly variable from one cell type to another one[13-17]. In addition, Stat3 has been described to have non-transcriptional roles in regulating cell migration[18] and mitochondrial electron transport chain[19, 20].

Recent studies have implicated Stat3 in the progression of CKD. Indeed, in several human and experimental nephropathies, Stat3 activation has been shown in different compartments of the damaged kidney, including tubular cells[21-28]. Interestingly, both *Stat3* haploinsufficiency and Stat3 pharmacological inhibition have been shown to decrease lesion progression in HIV-associated nephropathy[26], experimental diabetes[24] or ureteral obstruction[29]. Although these studies were conducted in specific experimental models, they point to Stat3 as an important mediator of CKD progression. However, the molecular mechanisms involved in the deleterious effect of Stat3 remain to be elucidated. Remarkably, a few studies have demonstrated that Stat3 is mechanistically involved in the communication between epithelial cells and fibroblasts[30-32]. Taking all these data together, we hypothesized that Stat3 orchestrates the communication between tubular and interstitial cells, leading to the development of interstitial fibrosis.

## RESULTS

### Tubular Stat3 activation precedes renal lesion development after nephron reduction

To investigate whether the activation of Stat3 is a common feature of CKD progression, we analyzed Stat3 ($Y^{706}$) phosphorylation after subtotal nephrectomy (Nx) in three mouse strains that differently react to Nx[33, 34]. We chose this model, since nephron reduction characterizes the evolution of most human CKD. Consequently, this model recapitulates many features of human CKD, including hypertension, proteinuria, glomerular and tubulo-interstitial lesions. Immunohistochemistry revealed p-Stat3 ($Y^{706}$) positive cells in the tubules and interstitium of the damaged kidneys of the lesion-prone FVB/N mice, but not in the remnant kidneys of the resistant C57BL/6 and B6D2F1 mice (**Figure 1A**). A time course analysis showed that the activation of Stat3 in tubular cells preceded the development of renal lesions 42 days after Nx (**Figure 1, B and C**). Sixty days after Nx, when frank renal lesions developed in FVB/N mice, Stat3 phosphorylation was still observed in renal tubules as well as in interstitial cells. In contrast, glomerular staining was rarely observed (data not shown). Analysis of serial sections stained for p-Stat3 ($Y^{706}$) and specific tubular markers revealed that Stat3 activation localized principally to the ascending loop of Henle and collecting duct at day 42 (**Figure 2**). Notably, 60 days after Nx, Stat3 phosphorylation was also observed in damaged proximal tubules (**Figure 2**).

### Tubular specific *Stat3* deletion reduces tubulo-interstitial lesions after nephron reduction

We then assessed the functional consequence of tubular Stat3 activation during CKD progression. Towards this aim, we first introduced the $Stat3^{flox}$ and $Ksp.creER^{T2}$ alleles in the lesion-prone (FVB/N) genetic background[35, 36]. Then, we deleted *Stat3* specifically in tubular cells ($Stat3^{\Delta tub}$ mice) by crossing *Stat3* floxed adult mice ($Stat3^{flox}$) with the $Ksp.creER^{T2}$ deleter strain, which drives a tamoxifen dependent recombination of the floxed alleles in renal tubular

cells[35]. Indeed, by crossing these mice with a reporter *Rosa26.lacZ* strain, we confirmed that the expression of LacZ activity was exclusively located to renal tubules with a less efficient targeting of its proximal parts (**Supplemental Figure 1**). PCR experiments on different organs confirmed the kidney specific *Stat3*$^{flox}$ allele recombination (*Stat3*$^{\Delta tub}$ mice) (**Figure 3A**). Two weeks after tamoxifen treatment, the amount of Stat3 protein was reduced by more than 50% in kidneys of *Stat3*$^{\Delta tub}$ mice as compared to *Stat3*$^{flox}$ littermates (**Figure 3B**). Stat3 immunostaining confirmed the marked decrease of Stat3 expression in renal tubular cells (**Figure 3C**).

We next applied our experimental model of Nx to both *Stat3*$^{flox}$ and *Stat3*$^{\Delta tub}$ mice, two weeks after tamoxifen treatment. Notably, the selective inactivation of *Stat3* in tubular cells was sufficient to prevent Stat3 ($Y^{706}$) phosphorylation in whole kidney 60 days after Nx, indicating that the bulk of Stat3 activation occurs in tubular cells (**Figure 3D**). Consistently, the expression of *Socs3* mRNA, a well–characterized target of Stat3, was significantly decreased in *Stat3*$^{\Delta tub}$ mice as compared to *Stat3*$^{flox}$ littermates (**Figure 3E**). As expected, tubular *Stat3* invalidation had a significant impact on the development of tubular lesions after Nx. Indeed, the extent of tubular dilations was reduced by 35% in *Stat3*$^{\Delta tub}$ mice as compared to *Stat3*$^{flox}$ littermates (**Figure 4**). More strikingly, preventing Stat3 activation in tubular cells had a marked impact on interstitial fibrosis, which was three fold less severe in *Stat3*$^{\Delta tub}$ mice as compared to *Stat3*$^{flox}$ littermates (**Figure 4**). In contrast, glomerular lesions were mild and did not differ between the two mouse genotypes. Together these results indicate that Stat3 activation in tubular cells promotes interstitial fibrosis after Nx.

**Tubular Stat3 does not affect tubular cell turnover or functional differentiation**

Tubular dilation is frequently the consequence of increased cell proliferation or impaired apoptosis[37, 38]. To get further insights into the mechanisms by which Stat3 promotes tubular dilations, we assessed tubular proliferation and apoptosis in mutant and control mice 90 days after Nx by using PCNA staining and TUNEL assay. Surprisingly, *Stat3* tubular invalidation prevented tubular dilation without impacting tubular cell proliferation or increasing cell apoptosis (**Supplemental Figure 2, A and B**).

In parallel, in order to determine if *Stat3* invalidation might impact tubular functions, we measured the relative expression of important transcript for proximal tubule (*Megalin, Pepck, Slc34a1 and Slc34a3*), thick ascending limb (*Slc12a1* and *Umod*), distal tubule (*Slc12a3* and *Calb1*) and collecting duct (*Scnn1*, *Aquaporin 2* and *Slc4a1*) functions. Among these genes, only the expression of *Megalin*, *Scnn1* (which codes the α subunit of the epithelial sodium channel) and *Slc4a1* (which codes anion exchanger 1) were reduced after Nx. More importantly, tubular *Stat3* deletion did not impact the expression of any of these genes (**Supplemental Figure 3**).

**Tubular Stat3 activation promotes interstitial matrix and fibroblast accumulation**

We then sought to elucidate the mechanisms by which the activation of Stat3 in tubular cells influences the accumulation of matrix in the interstitium. In this aim, we first quantified the expression of the main collagen proteins known to accumulate during the fibrogenetic process and found that collagen I (*Col1a1*), III (*Col3a1*) and IV (*Col4a1*) alpha-1 chain mRNA expression was markedly reduced in that $Stat3^{\Delta tub}$ mice as compared to $Stat3^{flox}$ mice after Nx (**Figure 5A**). Alpha-smooth muscle actin-positive (α−sma+) interstitial fibroblasts are considered the main producers of collagen in damaged kidneys[39]. Interestingly, we observed that the number of α−sma+ cells was dramatically decreased in remnant kidneys of $Stat3^{\Delta tub}$

mice as compared to *Stat3*$^{flox}$ littermates (**Figure 5B**). In contrast, *Stat3* deletion did not prevent the increase of another distinct fibrogenic interstitial cell population, the S100a4+ cells[40] (**Figure 5C**). Recent fate tracing experiments performed in other experimental CKD models indicate that epithelial to mesenchymal transition does not significantly contribute to the expansion of the interstitial myofibroblastic population, which instead derives form renal pericytes and/or resident fibroblasts[41-43]. In line with these observations, we observed that α-sma+ cells frequently co-stained with the pericyte marker platelet-derived growth factor receptor β (Pdgfr-β) (**Figure 5D**). Of note, renal tubular cells remained constantly negative for α−sma staining after Nx. More importantly, localization analysis of α-sma, Pdgfr-β and p-Stat3 ($Y^{706}$) on serial sections revealed clusters of α−sma+/Pdgfr-β+ cells organized along tubules with p-Stat3+ nuclei (**Figure 5D**). As previously shown after unilateral ureteral obstruction[22], α−sma+/Pdgfr-β+ cells were also positive for p-Stat3 ($Y^{706}$). Collectively, these results suggest that, during CKD, tubular Stat3 stimulates the activation of interstitial fibroblasts, likely via the secretion of (a) paracrine factor(s).

**Identification of the potential Stat3 target genes involved in the tubulo-interstitial paracrine signal**

To identify the potential direct target genes of Stat3 that may mediate fibroblast activation, we took advantage of a method that we recently developed to predict Stat3 functional binding sites through comparative genomics[16]. Using this approach, we re-analyzed the results of a transcriptome profiling that we previously carried out in remnant kidneys from the lesion-prone FVB/N and lesion-resistant C57BL/6 mice. We identified 1815 transcripts whose expression significantly differed between FVB/N and C57BL/6 mice 60 days after Nx. Among them, 1069 were up-regulated in FVB/N remnant kidneys, whereas 746 were down-regulated. Interestingly, we observed an enrichment of Stat3 conserved binding sites (CBS) in the genes differentially expressed between the lesion-prone and the lesion-resistant mice

(**Figure 6A**). Consistent with the fact that Stat3 behaves mainly as a transcriptional activator[14], Stat3 CBS enrichment concerned preferentially the up-regulated genes. We next decided to focus our analysis on the 570 genes with a Stat3 CBS conserved in at least 4 species (**Figure 6B** and **Supplemental Table 1**). To refine our analysis we systematically retrieved Entrez Gene Database, UniprotKB database and MGI Phenotypes and Mutants Community Resources for the 570 genes and assessed their potential role in fibroblasts activation. Among them, we identified 16 genes encoding for paracrine molecules that could account for the tubulo-interstitial communication (**Table 1**).

**Tubular specific *Stat3* inactivation reduces the expression of distinct genes promoting extracellular matrix accumulation after nephron reduction**

Quantitative RT-PCR confirmed that six of the potential candidates were significantly altered in remnant kidneys of FVB/N mice 60 days after after Nx (**Figure 7**). Among these genes, only three showed Stat3 dependent up-regulation after Nx: *Lcn2*, *Pdgfb* and *Timp1* (**Figure 7**). Colocalization studies revealed that Lcn2, Timp-1 protein as well as *Pdgfb* mRNA localized to p-Stat3 ($Y^{706}$) positive tubular cells 60 days after Nx (**Figure 8, A, B and C**), supporting the hypothesis of a cell autonomous regulation by Stat3. The colocalization was however not found in all the tubular cells, indicating Stat3 independent expression of these genes and/or tubular reabsorption of secreted proteins. We then switched to an *in vitro* approach to test whether Lcn2, Timp-1 and Pdgfb are direct targets of Stat3 in renal tubular cells. In this aim, we treated mIMCD3 cells with three Stat3 activators of the interleukin 6 family: Oncostatin M (Osm), Leukemia inhibiting factor (Lif) and Interleukin-6 (IL-6). We used these three well-characterized activators of Stat3 because we found that their expression was specifically increased in remnant kidneys of FVB/N mice 60 days after surgery as compare to sham-operated mice (**Supplemental Figure 4**). Of these three cytokines, Osm induced the strongest phosphorylation of Stat3 *in vitro* (**Figure 8D**), which correlated with the

strongest induction of *Socs3* mRNA expression (**Figure 8E**). Notably, Osm treatment resulted in a significant increase of *Lcn2*, *Timp-1* and *Pdgfb* mRNA (**Figure 8E**). To unequivocally determine if this activation was dependent by Stat3, we used lentiviral transduction of short hairpin RNA to knock-down *Stat3* expression (**Figure 8F**). In line with our hypothesis, we observed that *Stat3* knock-down blunted the up-regulation of *Lcn2*, *Timp-1* and *Pdgfb* transcript in response to Osm (**Figure 8G**).

**Lcn2 promotes collagen expression in tubular cells.**

Both Pdgfb and Timp-1 have been shown to induce fibroblasts proliferation[44-46]. In contrast, evidence regarding the fibrogenic potential of Lcn2 are scarce. Recently, Lcn2 was shown to enhance *Col1* mRNA expression in fibroblasts[47]. To assess if Lcn2 could modulate collagen production in renal tubular cells (mIMCD-3), we used lentiviral transduction of short hairpin RNA to knock-down *Lcn2* expression (**Figure 9A**). mIMCD-3 cells expressed both *Col1a1* and *Col4a1*, but not *Col3a1* (data not shown). Tubular *Lcn2* knock-down was associated with a reduction of both *Col1a1* and *Col4a1* mRNA expression (**Figure 9B**). Interestingly, these finding were relevant *in vivo*. In fact, we observed, in damaged kidneys of Nx mice, an increase of *Col4a1* deposition in the vicinity of tubules expressing Lcn2 (**Figure 9C**). In addition, *Col4a1* signal was preferentialy detected in the cytoplasm of Lcn2-positive cells. Together these results suggest that Lcn2 acts as a fibrogenic factor by promoting collegen synthesis by tubular cells.

## DISCUSSION

The accumulation of extracellular matrix in the renal interstitium plays a central role in CKD progression. Recent fate tracing experiments have identified activated α-sma+ interstitial fibroblast as the principal cell type responsible for matrix deposition into the interstitium[39, 43]. However, tubular cells are the primary target of critical factors implicated in CKD progression such as proteinuria, toxic injuries or mechanical stresses. The mechanisms translating tubular cell injuries to interstitial fibroblast activation remain unclear. By applying an experimental model of nephron reduction to mice carrying a specific deletion of *Stat3* in tubular cells, we have disclosed a novel paracrine network that is crucially involved in the communication between the damaged tubular cells and the surrounding fibroblasts during CKD progression. Mechanistically, tubular Stat3 activation triggered the activation of interstitial fibroblasts/pericytes, which ultimately lead to the development of interstitial fibrosis. Furthermore, we have discovered that Stat3 acts through the induction of a peculiar subset of profibrotic genes, i.e. *Lcn2, Pdgfb and Timp1*. Collectively, this work provides the first experimental evidence for a role of tubular cells in the development of renal fibrosis and identify in Stat3 a critical regulator.

Although several studies have demonstrated an activation of Stat3 in tubular cells in both human and experimental nephropathies[22-28], the functional consequences of such activation are still unknown. Our study points to tubular Stat3 activation as the first of a cascade of events leading the proliferation of the neighbouring fibroblasts and the subsequent development of interstitial fibrosis. After almost two decades of controversy, fate tracing experiments have firmly established that the majority of α-sma+ cells does not derive from tubular cells through epithelial-mesenchymal transition but rather from resident interstitial cells corresponding to renal fibroblasts and/or pericytes[41-43]. At the same time, several studies have clearly

demonstrated that activation of tubular cells parallels the development of interstitial fibrosis[48-50], suggesting that the interaction between these two compartments might play a crucial role in CKD progression. By showing that the selective inactivation of Stat3 in tubular cell prevented the development of interstitial fibrosis, our study provides direct evidence in favor of this idea. More importantly, we have deciphered a novel paracrine network between tubular and interstitial cells governed by Stat3 activation in the former cells. In this context, we have identified three potential soluble profibrotic effectors of tubular Stat3 activation: Lcn2, Pdgfb and Timp1. Several evidence support the idea that these molecules may be the critical triggers of the fibrogenetic process in this specific network. First, interstitial fibroblasts/pericytes constitutively express the β isoform of the Pdgf receptor and exogenous Pdgfb administration result in fibroblast activation and renal fibrosis[51]. In addition, pharmacologic inhibition of Pdgfb signaling reduces renal fibrosis in experimental CKD[52]. Second, we previously showed that the expression of Lcn2 (also named NGAL), a secreted molecule, which binds siderophore[53] is up-regulated in both human and rodent CKD[54]. Lcn2 has been shown to interact with the matrix metallopeptidase 9 (Mmp9)[55], a peptidase involved in kidney matrix turnover. Interestingly, *Lcn2* gene inactivation reduces the development of interstitial fibrosis after Nx[54]. Our results showing that Lcn2 increases collagen production in renal tubular cells provide further evidence for a direct link between Lcn2 and renal fibrosis. Finally, although genetic manipulations of Timp1 have led to contradictory results in experimental CKD[56, 57], it is likely that the marked reduction of Timp1 might partially contribute to the beneficial effect of *Stat3* deletion in Nx mice. In fact, it is acknowledged that the balance between matrix metalloproteases and matrix metalloprotease inhibitors synthesis determines the extent of matrix accumulation[58]. Beyond its direct impact on matrix degradation, Timp1 has been shown to promote fibroblast proliferation providing another potential pathophysiologic fibrogenic function for this molecule[45, 46].

An important corollary finding of this study is that tubular Stat3 induced the accumulation of interstitial matrix through the induction of a specific and original subset of profibrotic genes. Strikingly, Stat3 deletion impacted neither the expression of Tgf-β2 nor that of CTGF, a well-characterized profibrotic transcriptional target of canonical Tgf-β signaling, suggesting that Stat3 signals orthogonally to Tgf-β in this context[59]. Of note, the expression of several other profibrotic genes including endothelin 1 or fibronectin, that we showed increased after Nx, were also unaffected by *Stat3* deletion. Hence, it seems that the progression of renal fibrosis is fuelled by the intricacy of distinct transcriptional programs that can be independently targeted to reduce the extent of renal damage. Tgf-β signaling is to date the most studied contributor to the renal fibrosis and therapeutic strategies aiming at its inhibition have evolved to phase I and phase II clinical studies[60]. However, in other pathologic contexts, Tgf-β inhibition has recently been shown to be insufficiently effective and associated with significant side effects[61]. Our finding points at Stat3 inhibition as an alternative and/or a synergic therapeutic approach to Tgf-β inhibition in CKD.

A striking observation of this study is that the beneficial effect of *Stat3* deletion on tubular dilations was associated neither with a decrease of cell proliferation, nor with an increase of apoptosis. These results suggest that tubular Stat3 triggers tubular dilations through a mechanisms that is independent from proliferation or apoptosis and might involve planar cell polarity (PCP). In fact, it has been reported that a defect in the orientation of the mitotic spindle (oriented cell divsion) participates to tubular dilation[62]. Interestingly, during zebrafish gastrulation, Stat3 has been shown to control PCP signalling[63].

An unresolved question is the nature of the event(s) leading to Stat3 activation in tubular cells after nephron reduction. Important factors for CKD progression such as albuminuria and Epidermal Growth Factor Receptor (EGFR) activate Stat3 in cultured epithelial cells[64].

However, it is unlikely that these factors induce Stat3 activation in a cell autonomous manner in our model. Indeed, both albuminuria mediated tubular damage and EGFR activation occurs mainly in the proximal tubules whereas we detected Stat3 activation mainly in the distal part of the nephron[65, 66]. Moreover, the deleter *Ksp.creER*$^{T2}$ strain we used to inactivate *Stat3*$^{flox}$ allele in tubular cells principally targets the ascending loop of Henle and the collecting duct. Thus, the reduction of the interstitial fibrosis observed in this model likely reflects Stat3 function in the distal rather than in the proximal part of the nephron. In this context, the *bona fide* activator(s) of Stat3 in this segment remain to be identified. Interestingly, we observed that Oncostatin mRNA was up-regulated after Nx and that this cytokine stimulated the expression of Pdgfb, Timp-1 and Lcn2 in a Stat3 dependent manner in cultured renal epithelial cells. Whether or not Oncostatin plays the same role *in vivo* remains to be assessed.

In conclusion, this work established the critical role played by tubular cells in the development of interstitial fibrosis after nephron reduction. We have also identified Stat3 as a master gene of the paracrine molecular network linking tubular and interstitial compartment during CKD progression. Other studies have previously showed the deleterious impact of Stat3 activation in glomeruli[24, 26, 67, 68]. Therefore, Stat3 seems to be a promising therapeutic target for the maintenance of both the glomerular and tubulo-interstitial compartment during chronic kidney disease.

## METHODS

### Animals

Mice used for these studies were female FVB/N, C57BL/6 and C57BL/6xDBA2/F1 (B6D2F1) (Charles River), *Ksp.creER*$^{T2}$ mice[35, 36], *Stat3*$^{flox}$ mice[35, 36], and Rosa26LacZ mice (Jackson Laboratories). FVB/N *Stat3*$^{flox}$ and *Ksp.creER*$^{T2}$ were obtained by backcrossing heterozygous C57BL/6 *Stat3*$^{flox/+}$ and *Ksp.creER*$^{T2}$ mice on an FVB/N background for at least five generations before the first intercross. Animals were fed *ad libitum* and housed at constant ambient temperature in a 12-hour light cycle. Animal procedures were approved by the Departmental Director of "Services Vétérinaires de la Préfecture de Police de Paris" and by the ethical committee of the Paris Descartes University.

### Protocol

All experiments were performed on 9-week-old female mice. Protocols involving transgenic mice were performed on littermate mice. Mice were subjected to 75% nephrectomy (Nx) or sham operation (Sh), as previously described[33]. After surgery, mice were fed a defined diet containing 30% casein and 0.5% sodium. Several groups of mice were investigated in complementary studies. For Stat3 activation time course experiments, 6 mice were studied for each group (Sh B6D2F1, Nx B6D2F1, Sh FVB/N and Nx FVB/N) and each time point (30, 42 and 60 days after Nx). For microarray experiments, FVB/N and C57BL/6 mice were subjected to either sham operation or Nx (n = 4 for each group and genetic background) and sacrificed 60 days after surgery. For *Stat3* deletion experiments, we generated double transgenic FVB/N *Stat3*$^{flox/flox}$ X *Ksp.creER*$^{T2}$ mice (*Stat3*$^{\Delta tub}$ mice) that we compared to FVB/N *Stat3*$^{flox/flox}$ mice (*Stat3*$^{flox}$ mice). All mice were treated with tamoxifen at the dose of 7 mg per 40 g of body weight per day in ethanol:oil (10:1). Tamoxifen was delivered through intraperitoneal injection for five consecutive days. Two weeks after tamoxifen treatment, mice underwent either sham operation (n = 3 and 4 for *Stat3*$^{flox}$ and *Stat3*$^{\Delta tub}$ mice,

respectively) or Nx (n = 9 and 13 for *Stat3*$^{flox}$ and *Stat3*$^{\Delta tub}$ mice, respectively). Mice were sacrificed 90 days after surgery and the kidneys were harvested for analysis. This later time point was used because we noticed that tamoxifen treatment slowly delays renal lesion progression after Nx. For Rosa26 experiments, Rosa26 mice expressing (n = 4) or not (n = 2) the *Ksp.creER*$^{T2}$ transgene were induced by tamoxifen and sacrificed 2 weeks after tamoxifen treatment.

**Renal morphology**

Kidneys were fixed in 4% paraformaldehyde, paraffin embedded, and 4-$\mu$m sections were stained with Periodic Acid Schiff (PAS), Masson's trichrome, Hematoxylin Eosin (HE) and picro-sirius red. The degree of glomerular lesions and interstitial cellular infiltration was evaluated using a semiquantitative score methodology as previously described[33], with minor modifications[69]. Briefly, ten randomly selected cortical microscopic fields were scored. Glomerular lesions were evaluated on PAS-stained sections and graded from 0 to 3, according to the extent of sclerosis 0, 1, 2, 3 and 4 corresponding to glomerulosclerosis affecting less than 10%, 10 to 24%, 25 to 50% or more than 50% respectively. The degree of interstitial mononuclear cell infiltration was determined on H&E-stained sections using a 0-3 injury score: 0, 1, 2 and 3 corresponding to 0%, 1–10%, 10–30% and >30% involvement of the microscopic field, respectively. The degree of tubular dilation and interstitial fibrosis was automatically quantified using a Nikon digital camera Dx/m/1200 and NIS software (Laboratory Imaging Ltd). Ten randomly selected microscopic fields (X200) were scored. Surgical scars were excluded from analysis.

**Expression microarray**

Total RNA was extracted and purified from remnant kidneys of FVB/N and C57BL/6 using the Qiagen RNeasy Mini Kit (Qiagen) as suggested by the manufacturer. RNA was then quantified and inspected with a Bioanalyzer (Agilent Technologies). cDNAs were generated

and hybridized on mouse 430.2 Affymetrix chips (45101 probes) according to the Affymetrix protocol.

**Genome wide *in silico* analysis of potential Stat3 binding sites**

The method used for the construction of Stat3 positional weight matrix and the identification of Stat3 binding sites have been previously described[16]. The comparative genomic analysis was conducted as previously described with slight modifications: eight genomes were used for comparative analysis (*Mus musculus*, *Rattus norvegicus, Homo sapiens, Gallus gallus, Canis familiar, Danio rerio, Xenopus tropicalis, Tetraodon nigroviridis*) and only the binding sites located up to 15 kb upstream of the Transcription Start Site (TSS) were considered for further analysis.

**Quantitative RT-PCR**

mRNA was detected in mouse kidneys by quantitative RT-PCR using ABI PRISM 7700 Sequence Detection system (Applied Biosystems). *Rpl13* was used as the normalization controls. Primers (Eurogentec) are listed in **Supplemental Table 2.**

**Western blot**

Western blot were performed as previously described[70]. Primary antibodies used were: rabbit polyclonal anti-Stat3 (Cell Signaling Technology), rabbit monoclonal anti-p-Stat3 ($Y^{706}$) (Cell Signaling Technology), mouse monoclonal anti-α-tubulin antibody (Sigma-Aldrich), goat anti-Lcn2 antibodies (R&D system) at 1:2000 and mouse monoclonal anti-β-tubulin antibody (Sigma-Aldrich).

**Immunohistochemistry, immunofluorescence and β-galacosidase staining**

For immunohistochemistry, 4-μm sections of paraffin-embedded kidneys were submitted to the appropriate antigen retrieval. Then, sections were incubated with rabbit monoclonal anti-p-Stat3 ($Y^{706}$) antibodies (Cell Signaling Technology) at 1:100, anti-Stat3 rabbit polyclonal antibodies (Cell Signaling Technology), mouse anti-α–smooth muscle actin antibodies

(Dako) at 1:10000, rabbit anti-S100a4 antibodies (Abcam) at 1:200, goat anti-Tamm-Horsfall antibodies (Biogenesis) at 1:200, rabbit anti-Aquaporin 2 antibodies (Sigma-Aldrich) 1:400, goat anti-Lcn2 antibodies (R&D systems) at 1:300, mouse anti-Timp-1 antibodies (Pierce) at 1:100, rabbit anti-collagen IV alpha chain 1 (Novusbio) at 1:100, followed by the appropriate secondary antibody. For colocalization experiments with tubular markers, 4-mm serial sections of paraffin-embedded kidneys were used. Proximal tubules were stained using biotinylated-Lotus Tetragonolobus Lectin (Vector) at 1:50 followed by HRP-labeled streptavidin at 1:1000. β-galacosidase staining was performed as previously described[71]. All immunofluorescence co-localization studies were analyzed using an Axio-observer Z1 microscope with an ApoTome2 module (Zeiss), with the exception of Col4α1 and lcn2 co-staining, which was analyzed using a LSM 700 confocal microscope (Zeiss).

**Pdgfb *in situ* Hybridisation**

Murine Pdgfb chain cDNA cloned into pBluescript.SK (a kind gift from Cecilia Bondjers, Gottenberg University, Sweden) was linearized with XbaI (anti-sense probe) or HindIII (sense probe) and labelled RNA probes were synthesized with T7 RNA polymerase (anti-sense probe) or T3 RNA polymerase (sense probe) using dNTP mix containing digoxigenin-labelled uridine-triphosphate as substrate (Roche). *In situ* hybridization was carried out on 8 $\mu$m paraffin embedded sections. Sections were permeabilized in 0.2 N hydrochloric acid, digested with 10 μg/ml proteinase K (Roche), acetylated in 0.5% acetic anhydride and then hybridized overnight at 65 °C with 1 $\mu$g/ml of RNA probe. After washings, the slides were blocked in 10% goat serum and digoxin was revealed with anti-digoxigenin antibodies (Roche) at 1:1500, followed with nitroblue tetrazolium/bromochloroindolylphosphate (NBT/BCIP) AP substrate solution (Roche).

**Cell culture**

Mouse inner medulla collecting duct (mIMCD-3) cells were grown in DMEM/HamF12 (Gibco) medium containing 10% Fetal Bovine Serum (FBS, Sigma). To obtain optimal cellular differentiation and polarization, cells were plated at confluence on transwell 0.4-μm polycarbonate filters (Corning) and cultured for a minimum of 5 days. Prior to experiments, cells were starved in a serum free medium overnight. Then cells were exposed for 24h to Oncostatin (Osm, 20 ng/ml, R&D Systems), Lif (100 ng/ml, Life Technologies) or IL-6 (100 ng/ml, Life Technologies).

For stable cell lines, mIMCD-3 cells expressing shRNA against *Stat3* or *Lcn2* were generated as follows. Lentiviral shRNA plasmids for *Stat3* were obtained from Sigma-Aldrich. We used a target set of five clones with pLKO.1-puro as a backbone (TRCN0000071453, TRCN0000071454, TRCN0000071456, TRCN0000301878, TRCN0000301880 for Stat3 and TRCN0000425227, TRCN0000432763, TRCN0000425363, TRCN0000431679, TRCN0000055328 for Lcn2). The lentiviral particles were produced by cotransfection of HEK293T cells with three plasmids (pMD2G, psPAX2 and the shRNA vector) using lipofectamine 2000 (Lifetechnologies). Cells were infected in the presence of 8 μg/ml polybrene overnight and were selected 2 days after viral transduction in puromycin (2 μg/ml). Lentiviral constructs were selected for the subsequent experiments according to *Stat3* or *Lcn2* protein reduction as evaluated by western blot analysis.

**Data analysis and statistics**

Data were expressed as means ± SEM. Differences between the experimental groups were evaluated using ANOVA, followed when significant ($P < 0.05$) by the Tukey-Kramer test. When only two groups were compared, Student T-test or Mann-Whitney test were used as appropriate. For microarray experiments, results are expressed as a Log2 of the ratio Cy5/Cy3. Genes with a false-discovery rate (FDR) < 0.05 (using the Benjamini-Hochberg

procedure) and a fold change (FC) > 1.5 were considered significant. The statistical analysis was performed using Graphpad Prism Software.

**ACKNOWLEDGMENTS**

We thank Pauline Barre, Sophie Berissi, Noemi Gadessaud, Christine Bole and the LEAT, Histology and Genomics Platforms for technical assistance. We thank Denise Laouari for discussion. We are grateful to Cecilia Bondjers (Gottenberg University, Sweden) and to Noel Lammande (College de France, Paris, France) for anti-Pdgfb probe. This work was supported by INSERM, Université Paris Descartes, AP-HP, Agence Nationale Recherche, Fondation de la Recherche Médicale, pRED Roche Laboratories (Basel), Institut Roche de Recherche et Médecine Translationnelle (Paris).

## CONFLICTS OF INTEREST

The authors declare they have not conflict of interest.

**REFERENCES**


1. Zhang, QL, Rothenbacher, D: Prevalence of chronic kidney disease in population-based studies: systematic review. *BMC Public Health,* 8**:** 117, 2008.

2. Go, AS, Chertow, GM, Fan, D, McCulloch, CE, Hsu, CY: Chronic kidney disease and the risks of death, cardiovascular events, and hospitalization. *The New England journal of medicine,* 351**:** 1296-1305, 2004.

3. Wen, CP, Cheng, TY, Tsai, MK, Chang, YC, Chan, HT, Tsai, SP, Chiang, PH, Hsu, CC, Sung, PK, Hsu, YH, Wen, SF: All-cause mortality attributable to chronic kidney disease: a prospective cohort study based on 462 293 adults in Taiwan. *Lancet,* 371**:** 2173-2182, 2008.

4. Brenner, BM: Adaptation of glomerular forces and flows to renal injury. *Yale J Biol Med,* 51**:** 301-305, 1978.

5. Risdon, RA, Sloper, JC, De Wardener, HE: Relationship between renal function and histological changes found in renal-biopsy specimens from patients with persistent glomerular nephritis. *Lancet,* 2**:** 363-366, 1968.

6. Coppo, R, D'Amico, G: Factors predicting progression of IgA nephropathies. *J Nephrol,* 18**:** 503-512, 2005.

7. Seron, D, Moreso, F: Protocol biopsies in renal transplantation: prognostic value of structural monitoring. *Kidney Int,* 72**:** 690-697, 2007.

8. Kramann, R, Dirocco, DP, Maarouf, OH, Humphreys, BD: Matrix Producing Cells in Chronic Kidney Disease: Origin, Regulation, and Activation. *Current pathobiology reports,* 1, 2013.

9. Santos, CI, Costa-Pereira, AP: Signal Transducers and Activators of Transcription - from cytokine signalling to cancer biology. *Biochim Biophys Acta*, 2011.

10. Reich, NC, Liu, L: Tracking STAT nuclear traffic. *Nat Rev Immunol,* 6**:** 602-612, 2006.

11. Frank, DA: STAT3 as a central mediator of neoplastic cellular transformation. *Cancer letters,* 251**:** 199-210, 2007.

12. Takeda, K, Noguchi, K, Shi, W, Tanaka, T, Matsumoto, M, Yoshida, N, Kishimoto, T, Akira, S: Targeted disruption of the mouse Stat3 gene leads to early embryonic lethality. *Proc Natl Acad Sci U S A,* 94**:** 3801-3804, 1997.

13. Kidder, BL, Yang, J, Palmer, S: Stat3 and c-Myc genome-wide promoter occupancy in embryonic stem cells. *PLoS One,* 3**:** e3932, 2008.

14. Langlais, D, Couture, C, Balsalobre, A, Drouin, J: Regulatory network analyses reveal genome-wide potentiation of LIF signaling by glucocorticoids and define an innate cell defense response. *PLoS Genet,* 4**:** e1000224, 2008.

15. Ouyang, Z, Zhou, Q, Wong, WH: ChIP-Seq of transcription factors predicts absolute and differential gene expression in embryonic stem cells. *Proc Natl Acad Sci U S A,* 106**:** 21521-21526, 2009.

16. Vallania, F, Schiavone, D, Dewilde, S, Pupo, E, Garbay, S, Calogero, R, Pontoglio, M, Provero, P, Poli, V: Genome-wide discovery of functional transcription factor binding sites by comparative genomics: the case of Stat3. *Proc Natl Acad Sci U S A,* 106**:** 5117-5122, 2009.

17. Choy, MK, Movassagh, M, Siggens, L, Vujic, A, Goddard, M, Sanchez, A, Perkins, N, Figg, N, Bennett, M, Carroll, J, Foo, R: High-throughput sequencing identifies STAT3 as the DNA-associated factor for p53-NF-kappaB-complex-dependent gene expression in human heart failure. *Genome Med,* 2**:** 37, 2010.

18. Gao, SP, Bromberg, JF: Touched and moved by STAT3. *Sci STKE,* 2006**:** pe30, 2006.

19. Gough, DJ, Corlett, A, Schlessinger, K, Wegrzyn, J, Larner, AC, Levy, DE: Mitochondrial STAT3 supports Ras-dependent oncogenic transformation. *Science,* 324**:** 1713-1716, 2009.

20. Wegrzyn, J, Potla, R, Chwae, YJ, Sepuri, NB, Zhang, Q, Koeck, T, Derecka, M, Szczepanek, K, Szelag, M, Gornicka, A, Moh, A, Moghaddas, S, Chen, Q, Bobbili, S, Cichy, J, Dulak, J, Baker, DP, Wolfman, A, Stuehr, D, Hassan, MO, Fu, XY, Avadhani, N, Drake, JI, Fawcett, P, Lesnefsky, EJ, Larner, AC: Function of mitochondrial Stat3 in cellular respiration. *Science,* 323**:** 793-797, 2009.

21. Hernandez-Vargas, P, Lopez-Franco, O, Sanjuan, G, Ruperez, M, Ortiz-Munoz, G, Suzuki, Y, Aguado-Roncero, P, Perez-Tejerizo, G, Blanco, J, Egido, J, Ruiz-Ortega, M, Gomez-Guerrero, C: Suppressors of cytokine signaling regulate angiotensin II-activated Janus kinase-signal transducers and activators of transcription pathway in renal cells. *J Am Soc Nephrol,* 16**:** 1673-1683, 2005.

22. Kuratsune, M, Masaki, T, Hirai, T, Kiribayashi, K, Yokoyama, Y, Arakawa, T, Yorioka, N, Kohno, N: Signal transducer and activator of transcription 3 involvement in the development of renal interstitial fibrosis after unilateral ureteral obstruction. *Nephrology (Carlton),* 12**:** 565-571, 2007.

23. Arakawa, T, Masaki, T, Hirai, T, Doi, S, Kuratsune, M, Arihiro, K, Kohno, N, Yorioka, N: Activation of signal transducer and activator of transcription 3 correlates with cell proliferation and renal injury in human glomerulonephritis. *Nephrol Dial Transplant,* 23**:** 3418-3426, 2008.

24. Lu, TC, Wang, ZH, Feng, X, Chuang, PY, Fang, W, Shen, Y, Levy, DE, Xiong, H, Chen, N, He, JC: Knockdown of Stat3 activity in vivo prevents diabetic glomerulopathy. *Kidney Int,* 76**:** 63-71, 2009.

25. Berthier, CC, Zhang, H, Schin, M, Henger, A, Nelson, RG, Yee, B, Boucherot, A, Neusser, MA, Cohen, CD, Carter-Su, C, Argetsinger, LS, Rastaldi, MP, Brosius, FC, Kretzler, M: Enhanced expression of Janus kinase-signal transducer and activator of

transcription pathway members in human diabetic nephropathy. *Diabetes,* 58**:** 469-477, 2009.

26. Feng, X, Lu, TC, Chuang, PY, Fang, W, Ratnam, K, Xiong, H, Ouyang, X, Shen, Y, Levy, DE, Hyink, D, Klotman, M, D'Agati, V, Iyengar, R, Klotman, PE, He, JC: Reduction of Stat3 Activity Attenuates HIV-Induced Kidney Injury. *J Am Soc Nephrol*, 2009.

27. Ortiz-Munoz, G, Lopez-Parra, V, Lopez-Franco, O, Fernandez-Vizarra, P, Mallavia, B, Flores, C, Sanz, A, Blanco, J, Mezzano, S, Ortiz, A, Egido, J, Gomez-Guerrero, C: Suppressors of cytokine signaling abrogate diabetic nephropathy. *J Am Soc Nephrol,* 21**:** 763-772, 2010.

28. Leonhard, WN, van der Wal, A, Novalic, Z, Kunnen, SJ, Gansevoort, RT, Breuning, MH, de Heer, E, Peters, DJ: Curcumin inhibits cystogenesis by simultaneous interference of multiple signaling pathways: In vivo evidence from a Pkd1-deletion model. *Am J Physiol Renal Physiol*, 2011.

29. Pang, M, Ma, L, Gong, R, Tolbert, E, Mao, H, Ponnusamy, M, Chin, YE, Yan, H, Dworkin, LD, Zhuang, S: A novel STAT3 inhibitor, S3I-201, attenuates renal interstitial fibroblast activation and interstitial fibrosis in obstructive nephropathy. *Kidney Int,* 78**:** 257-268, 2010.

30. Lim, CP, Phan, TT, Lim, IJ, Cao, X: Cytokine profiling and Stat3 phosphorylation in epithelial-mesenchymal interactions between keloid keratinocytes and fibroblasts. *The Journal of investigative dermatology,* 129**:** 851-861, 2009.

31. Lieblein, JC, Ball, S, Hutzen, B, Sasser, AK, Lin, HJ, Huang, TH, Hall, BM, Lin, J: STAT3 can be activated through paracrine signaling in breast epithelial cells. *BMC cancer,* 8**:** 302, 2008.

32. Cheng, N, Chytil, A, Shyr, Y, Joly, A, Moses, HL: Transforming growth factor-beta signaling-deficient fibroblasts enhance hepatocyte growth factor signaling in mammary carcinoma cells to promote scattering and invasion. *Mol Cancer Res,* 6**:** 1521-1533, 2008.

33. Pillebout, E, Burtin, M, Yuan, HT, Briand, P, Woolf, AS, Friedlander, G, Terzi, F: Proliferation and remodeling of the peritubular microcirculation after nephron reduction: association with the progression of renal lesions. *Am J Pathol,* 159**:** 547-560, 2001.

34. Laouari, D, Burtin, M, Phelep, A, Martino, C, Pillebout, E, Montagutelli, X, Friedlander, G, Terzi, F: TGF-alpha mediates genetic susceptibility to chronic kidney disease. *J Am Soc Nephrol,* 22**:** 327-335, 2011.

35. Lantinga-van Leeuwen, IS, Leonhard, WN, van der Wal, A, Breuning, MH, de Heer, E, Peters, DJ: Kidney-specific inactivation of the Pkd1 gene induces rapid cyst formation in developing kidneys and a slow onset of disease in adult mice. *Hum Mol Genet,* 16**:** 3188-3196, 2007.

36. Alonzi, T, Maritano, D, Gorgoni, B, Rizzuto, G, Libert, C, Poli, V: Essential role of STAT3 in the control of the acute-phase response as revealed by inducible gene inactivation [correction of activation] in the liver. *Mol Cell Biol,* 21**:** 1621-1632, 2001.

37. Ma, M, Tian, X, Igarashi, P, Pazour, GJ, Somlo, S: Loss of cilia suppresses cyst growth in genetic models of autosomal dominant polycystic kidney disease. *Nature genetics*, 2013.

38. Nishio, S, Hatano, M, Nagata, M, Horie, S, Koike, T, Tokuhisa, T, Mochizuki, T: Pkd1 regulates immortalized proliferation of renal tubular epithelial cells through p53 induction and JNK activation. *J Clin Invest,* 115**:** 910-918, 2005.

39. Lin, SL, Kisseleva, T, Brenner, DA, Duffield, JS: Pericytes and perivascular fibroblasts are the primary source of collagen-producing cells in obstructive fibrosis of the kidney. *Am J Pathol,* 173**:** 1617-1627, 2008.

40. Le Hir, M, Hegyi, I, Cueni-Loffing, D, Loffing, J, Kaissling, B: Characterization of renal interstitial fibroblast-specific protein 1/S100A4-positive cells in healthy and inflamed rodent kidneys. *Histochemistry and cell biology,* 123**:** 335-346, 2005.

41. Humphreys, BD, Lin, SL, Kobayashi, A, Hudson, TE, Nowlin, BT, Bonventre, JV, Valerius, MT, McMahon, AP, Duffield, JS: Fate tracing reveals the pericyte and not epithelial origin of myofibroblasts in kidney fibrosis. *Am J Pathol,* 176**:** 85-97, 2010.

42. Asada, N, Takase, M, Nakamura, J, Oguchi, A, Asada, M, Suzuki, N, Yamamura, K, Nagoshi, N, Shibata, S, Rao, TN, Fehling, HJ, Fukatsu, A, Minegishi, N, Kita, T, Kimura, T, Okano, H, Yamamoto, M, Yanagita, M: Dysfunction of fibroblasts of extrarenal origin underlies renal fibrosis and renal anemia in mice. *J Clin Invest,* 121**:** 3981-3990, 2011.

43. LeBleu, VS, Taduri, G, O'Connell, J, Teng, Y, Cooke, VG, Woda, C, Sugimoto, H, Kalluri, R: Origin and function of myofibroblasts in kidney fibrosis. *Nat Med,* 19**:** 1047-1053, 2013.

44. Chen, YT, Chang, FC, Wu, CF, Chou, YH, Hsu, HL, Chiang, WC, Shen, J, Chen, YM, Wu, KD, Tsai, TJ, Duffield, JS, Lin, SL: Platelet-derived growth factor receptor signaling activates pericyte-myofibroblast transition in obstructive and post-ischemic kidney fibrosis. *Kidney Int,* 80**:** 1170-1181, 2011.

45. Lu, Y, Liu, S, Zhang, S, Cai, G, Jiang, H, Su, H, Li, X, Hong, Q, Zhang, X, Chen, X: Tissue inhibitor of metalloproteinase-1 promotes NIH3T3 fibroblast proliferation by activating p-Akt and cell cycle progression. *Mol Cells,* 31**:** 225-230, 2011.

46. Lovelock, JD, Baker, AH, Gao, F, Dong, JF, Bergeron, AL, McPheat, W, Sivasubramanian, N, Mann, DL: Heterogeneous effects of tissue inhibitors of matrix metalloproteinases on cardiac fibroblasts. *Am J Physiol Heart Circ Physiol,* 288**:** H461-468, 2005.

47. Tarjus, A, Martinez-Martinez, E, Amador, C, Latouche, C, El Moghrabi, S, Berger, T, Mak, TW, Fay, R, Farman, N, Rossignol, P, Zannad, F, Lopez-Andres, N, Jaisser, F: Neutrophil Gelatinase-Associated Lipocalin, a Novel Mineralocorticoid Biotarget, Mediates Vascular Profibrotic Effects of Mineralocorticoids. *Hypertension,* 66**:** 158-166, 2015.

48. Ma, FY, Flanc, RS, Tesch, GH, Han, Y, Atkins, RC, Bennett, BL, Friedman, GC, Fan, JH, Nikolic-Paterson, DJ: A pathogenic role for c-Jun amino-terminal kinase signaling in renal fibrosis and tubular cell apoptosis. *J Am Soc Nephrol,* 18**:** 472-484, 2007.

49. Yang, L, Besschetnova, TY, Brooks, CR, Shah, JV, Bonventre, JV: Epithelial cell cycle arrest in G2/M mediates kidney fibrosis after injury. *Nat Med,* 16**:** 535-543, 531p following 143, 2010.

50. Prunotto, M, Budd, DC, Gabbiani, G, Meier, M, Formentini, I, Hartmann, G, Pomposiello, S, Moll, S: Epithelial-mesenchymal crosstalk alteration in kidney fibrosis. *J Pathol,* 228**:** 131-147, 2012.

51. Tang, WW, Van, GY, Qi, M: Myofibroblast and alpha 1 (III) collagen expression in experimental tubulointerstitial nephritis. *Kidney Int,* 51**:** 926-931, 1997.

52. Ostendorf, T, Eitner, F, Floege, J: The PDGF family in renal fibrosis. *Pediatr Nephrol,* 27**:** 1041-1050, 2012.

53. Paragas, N, Qiu, A, Hollmen, M, Nickolas, TL, Devarajan, P, Barasch, J: NGAL-Siderocalin in kidney disease. *Biochim Biophys Acta,* 1823**:** 1451-1458, 2012.

54. Viau, A, El Karoui, K, Laouari, D, Burtin, M, Nguyen, C, Mori, K, Pillebout, E, Berger, T, Mak, TW, Knebelmann, B, Friedlander, G, Barasch, J, Terzi, F: Lipocalin 2 is essential for chronic kidney disease progression in mice and humans. *J Clin Invest*, 2010.

55. Bolignano, D, Donato, V, Lacquaniti, A, Fazio, MR, Bono, C, Coppolino, G, Buemi, M: Neutrophil gelatinase-associated lipocalin (NGAL) in human neoplasias: a new protein enters the scene. *Cancer letters,* 288**:** 10-16, 2010.

56. Cai, G, Zhang, X, Hong, Q, Shao, F, Shang, X, Fu, B, Feng, Z, Lin, H, Wang, J, Shi, S, Yin, Z, Chen, X: Tissue inhibitor of metalloproteinase-1 exacerbated renal interstitial fibrosis through enhancing inflammation. *Nephrol Dial Transplant,* 23**:** 1861-1875, 2008.

57. Kim, H, Oda, T, Lopez-Guisa, J, Wing, D, Edwards, DR, Soloway, PD, Eddy, AA: TIMP-1 deficiency does not attenuate interstitial fibrosis in obstructive nephropathy. *J Am Soc Nephrol,* 12**:** 736-748, 2001.

58. Ronco, P, Chatziantoniou, C: Matrix metalloproteinases and matrix receptors in progression and reversal of kidney disease: therapeutic perspectives. *Kidney Int,* 74**:** 873-878, 2008.

59. Phanish, MK, Winn, SK, Dockrell, ME: Connective tissue growth factor-(CTGF, CCN2)--a marker, mediator and therapeutic target for renal fibrosis. *Nephron Exp Nephrol,* 114**:** e83-92, 2010.

60. Decleves, AE, Sharma, K: Novel targets of antifibrotic and anti-inflammatory treatment in CKD. *Nat Rev Nephrol,* 10**:** 257-267, 2014.

61. Denton, CP, Merkel, PA, Furst, DE, Khanna, D, Emery, P, Hsu, VM, Silliman, N, Streisand, J, Powell, J, Akesson, A, Coppock, J, Hoogen, F, Herrick, A, Mayes, MD, Veale, D, Haas, J, Ledbetter, S, Korn, JH, Black, CM, Seibold, JR: Recombinant

human anti-transforming growth factor beta1 antibody therapy in systemic sclerosis: a multicenter, randomized, placebo-controlled phase I/II trial of CAT-192. *Arthritis and rheumatism,* 56**:** 323-333, 2007.

62. Fischer, E, Legue, E, Doyen, A, Nato, F, Nicolas, JF, Torres, V, Yaniv, M, Pontoglio, M: Defective planar cell polarity in polycystic kidney disease. *Nature genetics,* 38**:** 21-23, 2006.

63. Miyagi, C, Yamashita, S, Ohba, Y, Yoshizaki, H, Matsuda, M, Hirano, T: STAT3 noncell-autonomously controls planar cell polarity during zebrafish convergence and extension. *J Cell Biol,* 166**:** 975-981, 2004.

64. Nakajima, H, Takenaka, M, Kaimori, JY, Hamano, T, Iwatani, H, Sugaya, T, Ito, T, Hori, M, Imai, E: Activation of the signal transducer and activator of transcription signaling pathway in renal proximal tubular cells by albumin. *J Am Soc Nephrol,* 15**:** 276-285, 2004.

65. Terzi, F, Burtin, M, Hekmati, M, Federici, P, Grimber, G, Briand, P, Friedlander, G: Targeted expression of a dominant-negative EGF-R in the kidney reduces tubulo-interstitial lesions after renal injury. *J Clin Invest,* 106**:** 225-234, 2000.

66. Chen, J, Chen, JK, Nagai, K, Plieth, D, Tan, M, Lee, TC, Threadgill, DW, Neilson, EG, Harris, RC: EGFR signaling promotes TGFbeta-dependent renal fibrosis. *J Am Soc Nephrol,* 23**:** 215-224, 2012.

67. Dai, Y, Gu, L, Yuan, W, Yu, Q, Ni, Z, Ross, MJ, Kaufman, L, Xiong, H, Salant, DJ, He, JC, Chuang, PY: Podocyte-specific deletion of signal transducer and activator of transcription 3 attenuates nephrotoxic serum-induced glomerulonephritis. *Kidney Int,* 84**:** 950-961, 2013.

68. Gu, L, Dai, Y, Xu, J, Mallipattu, S, Kaufman, L, Klotman, PE, He, JC, Chuang, PY: Deletion of podocyte STAT3 mitigates the entire spectrum of HIV-1-associated nephropathy. *AIDS (London, England),* 27**:** 1091-1098, 2013.

69. Pillebout, E, Weitzman, JB, Burtin, M, Martino, C, Federici, P, Yaniv, M, Friedlander, G, Terzi, F: JunD protects against chronic kidney disease by regulating paracrine mitogens. *J Clin Invest,* 112**:** 843-852, 2003.

70. Lautrette, A, Li, S, Alili, R, Sunnarborg, SW, Burtin, M, Lee, DC, Friedlander, G, Terzi, F: Angiotensin II and EGF receptor cross-talk in chronic kidney diseases: a new therapeutic approach. *Nat Med,* 11**:** 867-874, 2005.

71. Verdeguer, F, Le Corre, S, Fischer, E, Callens, C, Garbay, S, Doyen, A, Igarashi, P, Terzi, F, Pontoglio, M: A mitotic transcriptional switch in polycystic kidney disease. *Nat Med,* 16**:** 106-110, 2010.

**FIGURE LEGENDS**

**Figure 1**: **Stat3 activation after nephron reduction in kidneys from lesion-resistant and lesion-prone mice**. (**A**) Upper panel: periodic acid schiff staining (PAS) of remnant kidneys from C57BL/6, B6D2F1 and FVB/N mice 60 days after 75% nephrectomy (Nx). Lower panel: representative p-Stat3 ($Y^{706}$) immunostaining in the same animals. Scale bar: 100 μm (n=6 per group). (**B)** Western blot of Stat3 ($Y^{706}$) phosphorylation of whole kidney lysates of sham-operated (Sh) and 75% nephrectomised (Nx) B6D2F1 and FVB/N mice 30 (n=6 in each group), 42 (n=5 in each group) and 60 (n=6 in each group) days after surgery. Data are means ± SEM. ANOVA followed by Tukey-Kramer test. Sh *versus* Nx mice: * $P < 0.05$, ** $P < 0.01$, *** $P < 0.001$; B6D2F1 *versus* FVB/N mice: # $P < 0.05$, ## $P < 0.01$, ### $P < 0.001$. (**C)** Representative p-Stat3 ($Y^{706}$) immunostaining of kidneys from the same animals. Because kidneys from Sh B6D2F1 and Sh FVB/N mice were indistinguishable, only a single Sh control is shown. These are representative image of at least 5 mice in each group. Scale bar: 100 μm.

**Figure 2: Localization of Stat3 activation during renal lesion development.** Upper panel**:** representative co-immunostaining experiments and quantification of p-Stat3 ($Y^{706}$) and specific tubular markers, Tamm-Horshfall [ascending loop of Henle and the distal convoluted tubule (blue arrow)], lotus tetragonolobus lectin [proximal tubules (black arrow)] and aquaporin 2 [collecting tubule (green arrow)] in FVB/N remnant kidneys 42 and 60 days after 75% subtotal nephrectomy (n=3 in each group)**.** Scale bar: 100 μm. Lower panel: quantification of the percentage of p-Stat3 positive tubules marked with each of the markers.

**Figure 3: Conditional inducible deletion of *Stat3* in renal tubules of adult mice.** (**A**) Detection of Stat3 wild type (wt), floxed (fl) and deleted (Δ) allele on genomic DNA from the indicated tissue of wild type, $Stat3^{fl/+}$, $Stat3^{fl/fl}$ ($Stat3^{flox}$) and $Stat3^{fl/fl}$ *Ksp.creER*$^{T2}$ ($Stat3^{\Delta tub}$) mice two weeks after tamoxifen treatment. (**B-C**) Analysis of renal Stat3 expression by

western-blot **(B)** and immunohistochemistry (**C)** in *Stat3*$^{flox}$ (n=3) and *Stat3*$^{\Delta tub}$ (n=4) mice two weeks after tamoxifen treatment. (**D-E)** Western blot analysis and quantification of Stat3 ($Y^{706}$) phosphorylation **(D)** and *Socs3* mRNA expression **(E)** in sham-operated (Sh) *Stat3*$^{flox}$ (n=3), Sh *Stat3*$^{\Delta tub}$ (n=4), 75% nephrectomized (Nx) *Stat3*$^{flox}$ (n=9) and Nx *Stat3*$^{\Delta tub}$ (n=10) mice 90 days after surgery. Data are means ± SEM. t-test (in B) or ANOVA followed by Tukey-Kramer test (in D and E). Sh *versus* Nx mice: * $P < 0.05$, ** $P < 0.01$; *Stat3*$^{flox}$ *versus* *Stat3*$^{\Delta tub}$ mice: # $P < 0.05$, ## $P < 0.01$. Scale Bar: 50 μm.

**Figure 4: Tubular *Stat3* inactivation reduces tubulo-interstitial lesions after nephron reduction.** Morphology and lesion scores of kidneys from sham-operated (Sh) *Stat3*$^{flox}$ (n=3) and *Stat3*$^{\Delta tub}$ (n=4) mice and 75% nephrectomized (Nx) *Stat3*$^{flox}$ (n=9) and *Stat3*$^{\Delta tub}$ (n=13) mice 90 days after surgery. Data are means ± SEM. ANOVA followed by Tukey-Kramer test. Sh *versus* Nx mice: * $P < 0.05$, ** $P < 0.01$; *Stat3*$^{flox}$ *versus* *Stat3*$^{\Delta tub}$ mice: # $P < 0.05$, ## $P < 0.01$. Scale Bar: 100 μm.

**Figure 5: Tubular *Stat3* inactivation reduces interstitial collagen content and α-sma+ fibroblasts density after nephron reduction. (A)** Quantitative RT-PCR of renal collagen mRNA content in kidneys from sham-operated (Sh) *Stat3*$^{flox}$ (n=3) and *Stat3*$^{\Delta tub}$ (n=4) mice and 75% nephrectomized (Nx) *Stat3*$^{flox}$ (n=9) and *Stat3*$^{\Delta tub}$ (n=13) mice 90 days after surgery. (**B)** Representative α-sma immunostaining and quantification of α-sma+ cell density in sham-operated (Sh) *Stat3*$^{flox}$ (n=3) and *Stat3*$^{\Delta tub}$ (n=4) mice and 75% nephrectomized (Nx) *Stat3*$^{flox}$ (n=9) and *Stat3*$^{\Delta tub}$ (n=13) mice 90 days after surgery. (**C)** Representative S100a4 immunostaining and quantification of S100a4+ cell density of the same animals. (**D**) Representative colocalization between Pdgfr-β and α-sma (upper) and p-Stat3 ($Y^{706}$) and α-sma (lower) on serial sections of remnant kidneys of FVB/N mice 60 days after Nx**.** Data are means ± SEM. ANOVA followed by Tukey-Kramer test. Sh *versus* Nx mice: * $P < 0.05$,

** P < 0.01, *** P < 0.001; *Stat3*$^{flox}$ *versus* *Stat3*$^{\Delta tub}$ mice: # P < 0.05, ## P < 0.01, ### P < 0.001. Scale Bars: 50 μm.

**Figure 6**: **Potential Stat3 target genes during renal lesion development. (A)** Comparison of the frequency of predicted Stat3 binding sites in whole mouse genome (grey) and in the genes differentially expressed by C57BL/6 (n=4) and FVB/N (n=4) remnant kidneys 60 days after 75% nephrectomy (Nx). The green histogram shows all the differentially expressed genes (either up or down regulated in FVB/N mice as compared to C57BL/6 animals), while the red and the blue histograms concern only the genes up and down regulated in FVB/N as compared to C57BL/6 mice, respectively. (**B)** Schematic representation of the intersection between the genes with Stat3 binding sites conserved at least in 4 species and the genes differentially expressed between C57BL/6 and FVB/N remnant kidneys 60 days after Nx.

**Figure 7: Tubular *Stat3* inactivation affects the expression of specific paracrine fibrogenic factors after nephron reduction.** Quantitative RT-PCR of the 16 potential paracrine profibrotic Stat3 targets in sham-operated (Sh) *Stat3*$^{flox}$ (n=3) and *Stat3*$^{\Delta tub}$ (n=4) mice and 75% nephrectomized (Nx) *Stat3*$^{flox}$ (n=9) and *Stat3*$^{\Delta tub}$ (n=13) mice 90 days after surgery. All relative expression are normalized to Rpl13. Data are means ± SEM. ANOVA followed by Tukey-Kramer test. Sh *versus* Nx mice: * P < 0.05, ** P < 0.01, *** P < 0.001; *Stat3*$^{flox}$ *versus* *Stat3*$^{\Delta tub}$ mice: # P < 0.05, ## P < 0.01, ### P < 0.001.

**Figure 8: Stat3 regulates the expression of Lcn2, Timp1 and Pdgfb in renal tubular cells.** (**A**) Co-localization between p-Stat3 ($Y^{706}$) and Lcn2 in the remnant kidney of FVB/N mice 60 days after 75% subtotal nephrectomy (Nx). Scale Bar: 50 μm (**B**) Immunostaining of p-Stat3 ($Y^{706}$) (upper panel) and Timp1 (lower panel) on serial kidney sections from FVB/N mice 60 days after Nx. Scale Bar: 100 μm. (**C**) Immunostaining of p-Stat3 ($Y^{706}$) (upper panel) and *in situ* hybridization of Pdgfb mRNA (lower panel) on kidney serial sections from FVB/N mice 60 days after Nx. Scale Bar: 100 μm. (**D-E**) Western-blot of Stat3 ($Y^{706}$) phosphorylation (**D**)

and quantitative RT-PCR of *Socs3, Lcn2, Timp1* and Pdgfb mRNA (**E**) from mIMCD3 cells treated with oncostatin M (Osm), leukemia inhibiting factor (Lif), interleukin-6 (IL-6) or vehicle (Veh). (**F**) Western blot of Stat3 from mIMCD3 transduced with a short hairpin RNA targeting Stat3 (Stat3) or a scramble control (Scr). (**G**) Quantitative RT-PCR of *Socs3, Lcn2, Timp1* and *Pdgfb* mRNA expression in mIMCD3 transducted with a short hairpin RNA targeting Stat3 or a scramble control and treated with Osm or Veh. All relative expression are normalized to *Rpl13*. Data are means ± SEM. ANOVA followed by Tukey-Kramer test: Veh *versus* Osm, Lif or IL-6 treated cells: * $P < 0.05$, ** $P < 0.01$, *** $P < 0.001$; Cells transduced with a Stat3 Sh RNA versus a scramble Sh RNA: # $P < 0.05$, ## $P < 0.01$, ### $P < 0.001$.

**Figure 9: Lcn2 promotes collagen expression in renal tubular cells.** (A) Western blot analysis of Lcn2 expression in mIMCD3 cells transduced with either a short hairpin RNA targeting Lcn2 (Lcn2) or a scramble control (Scr). (B) Quantitative RT-PCR of *Col1a1* and *Col4a1* mRNA expression in mIMCD3 cells transduced with either a short hairpin RNA targeting Lcn2 (Lcn2) or a scramble control. Data are means ± SEM. Paired T-test: ** $P < 0.01$. (C) Representative confocal images of kidney sections from sham-operated (Sh; n=4) or 75% nephrectomized (Nx; n=6) FVB/N mice 60 days after surgery stained with Lcn2 and Col4a1 chain specific antibodies. Scale bar: 20 μm.

**Table 1**: Potential Stat3 paracrine targets involved tubulo-interstitial communication.

| Gene Symbol | Name | Fold variation FVB/N vs C57Bl/6 | Stat3 binding sites conservation |
|---|---|---|---|
| Lcn2 | lipocalin 2 | 6.52 | 4 species |
| Edn1 | endothelin 1 | 4.07 | 4 species |
| Cyr61 | cysteine-rich, angiogenic inducer, 61 | 3.94 | 4 species |
| Fst | follistatin | 3.70 | 6 species |
| Timp1 | tissue inhibitor of metalloproteinase 1 | 3.27 | 4 species |
| Tgm1 | transglutaminase 1 | 2.80 | 4 species |
| Tgfb2 | transforming growth factor, beta 2 | 2.43 | 4 species |
| Ctgf | connective tissue growth factor | 2.21 | 4 species |
| Adm | adrenomedullin | 2.11 | 4 species |
| Plau | plasminogen activator, urokinase | 2,04 | 4 species |
| Tagln2 | transgelin 2 | 1.71 | 4 species |
| Agt | angiotensinogen (serpin peptidase inhibitor, clade A, member 8) | 1.63 | 5 species |
| Pdgfb | platelet-derived growth factor beta polypeptide | 1.53 | 4 species |
| Angpt1 | angiopoietin 1 | 0.64 | 5 species |
| Enpp2 | ectonucleotide pyrophosphatase/phosphodiesterase 2 (autotaxin) | 0.51 | 4 species |
| Sfrp1 | secreted frizzled-related protein 1 | 0.30 | 4 species |

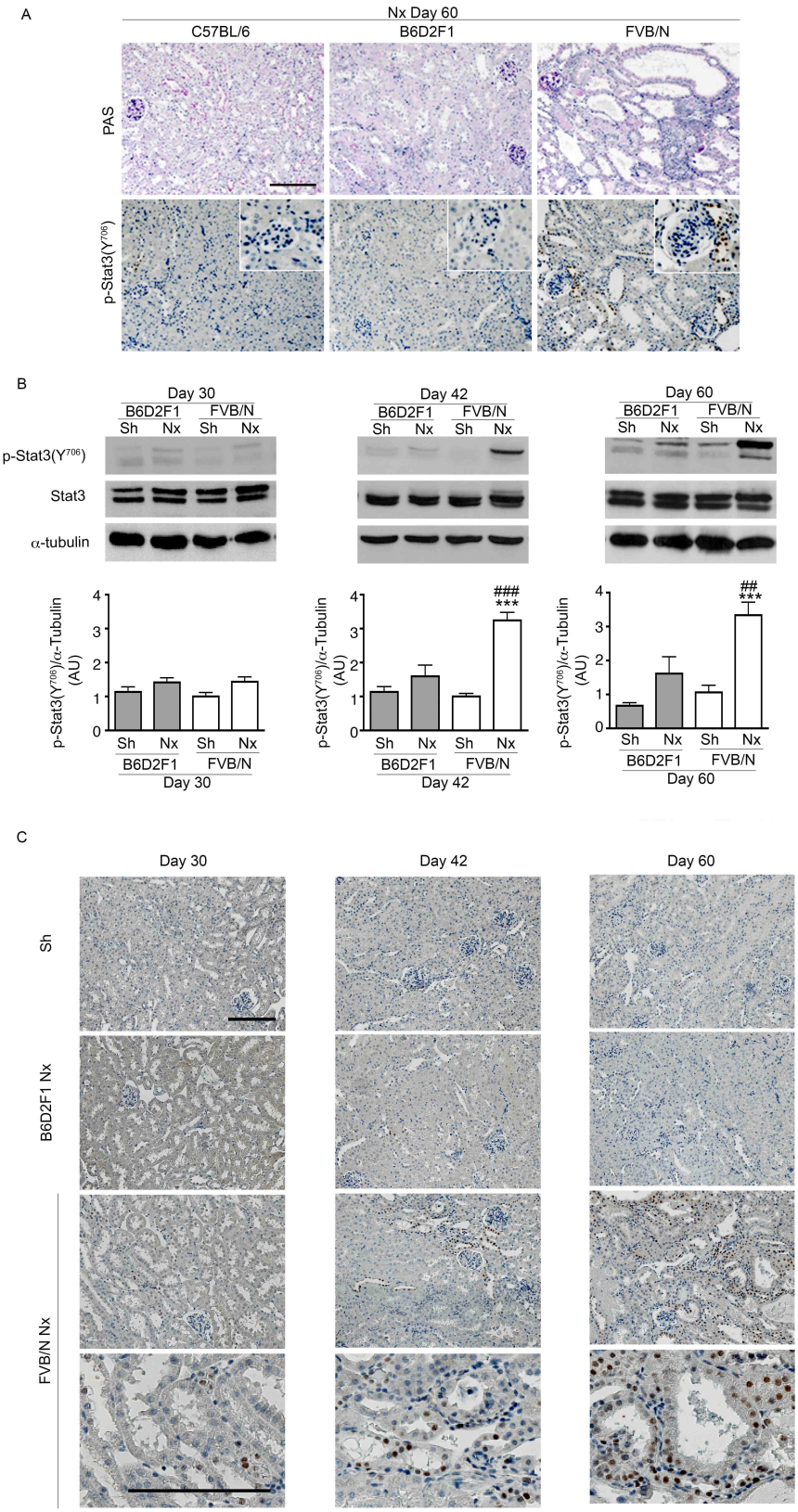
A
Nx Day 60
C57BL/6
B6D2F1
FVB/N
PAS
p-Stat3(Y706)
B
Day 30
Day 42
Day 60
B6D2F1
FVB/N
Sh
Nx
p-Stat3(Y706)
Stat3
α-tubulin
p-Stat3(Y706)/α-Tubulin (AU)
###
***
##
C
Day 30
Day 42
Day 60
Sh
B6D2F1 Nx
FVB/N Nx

Figure 1

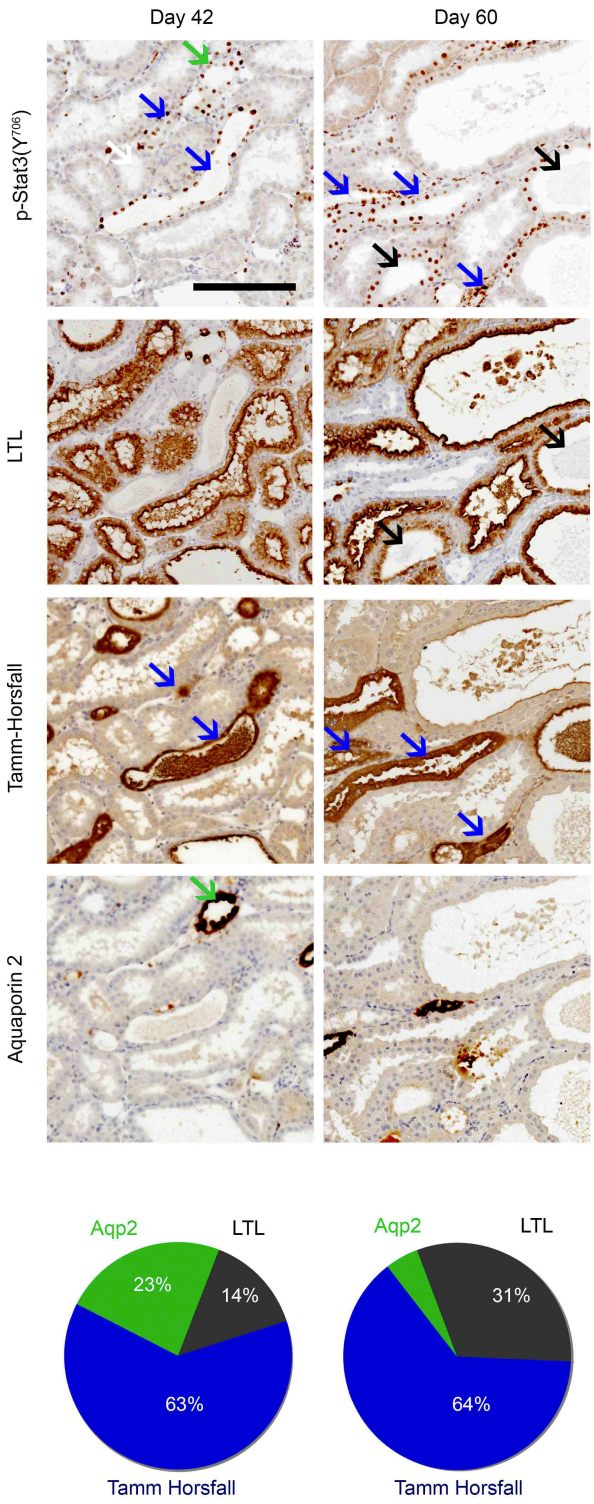
Day 42
Day 60
p-Stat3(Y705)
LTL
Tamm-Horsfall
Aquaporin 2
Aqp2
LTL
23%
14%
63%
Tamm Horsfall
Aqp2
LTL
31%
64%
Tamm Horsfall

Figure 2

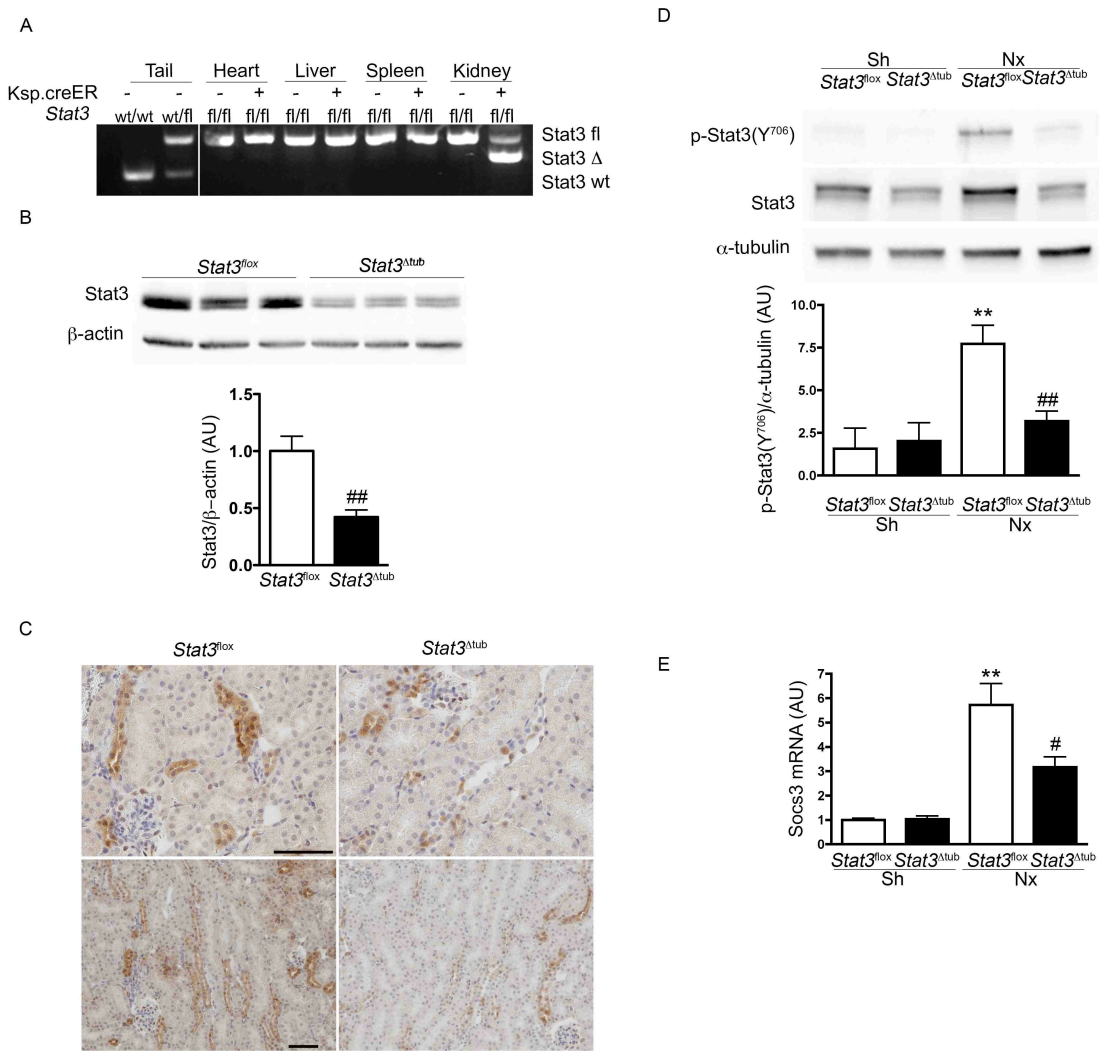
A
Tail
Heart
Liver
Spleen
Kidney
Ksp.creER
Stat3
wt/wt
wt/fl
fl/fl
Stat3 fl
Stat3 Δ
Stat3 wt
B
Stat3flox
Stat3Δtub
Stat3
β-actin
Stat3/β–actin (AU)
C
D
Sh
Nx
p-Stat3(Y706)
α-tubulin
p-Stat3(Y706)/α-tubulin (AU)
E
Socs3 mRNA (AU)

Figure 3

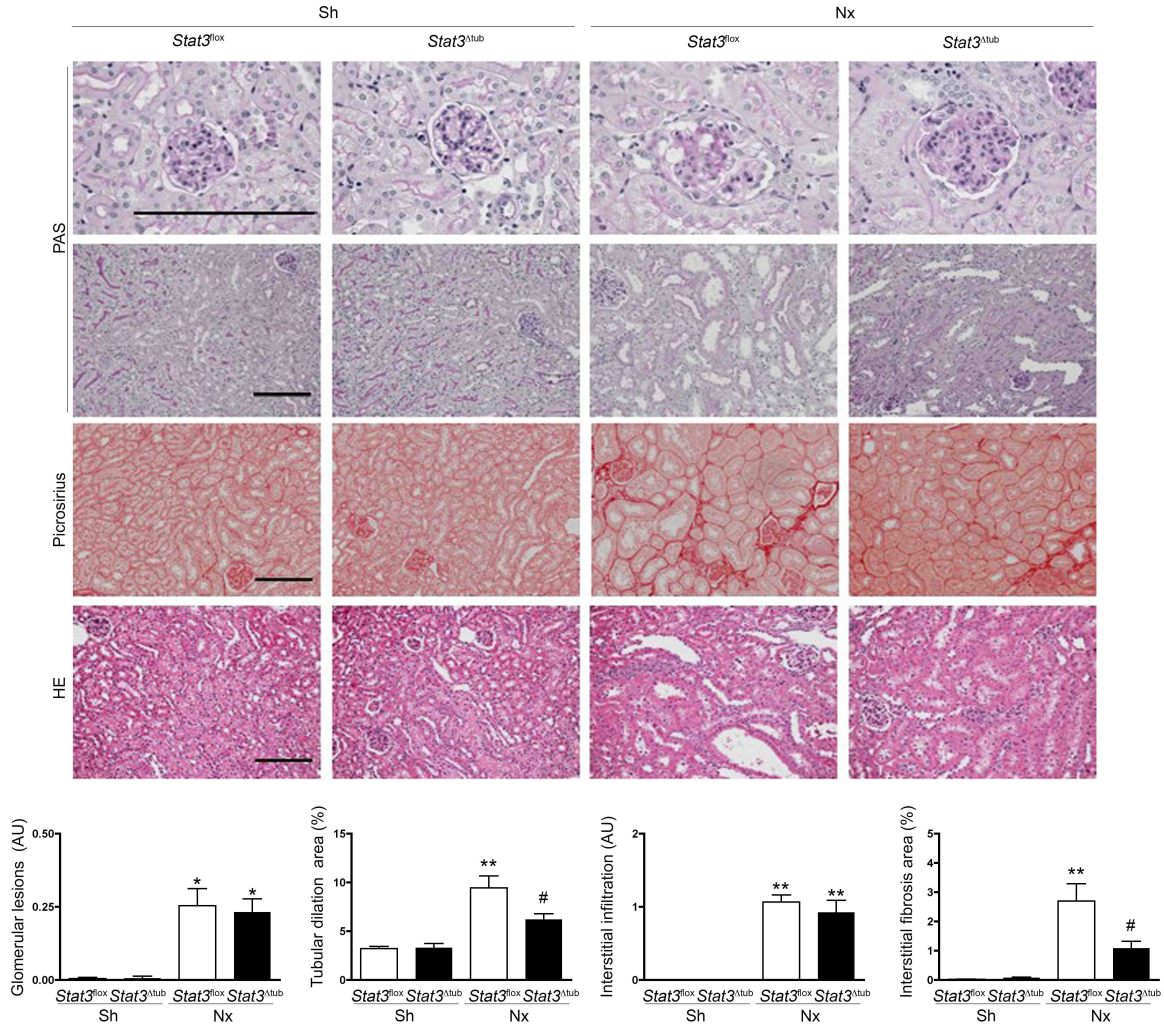
Sh
Nx
Stat3flox
Stat3Δtub
PAS
Picrosirius
HE
Glomerular lesions (AU)
Tubular dilation area (%)
Interstitial infiltration (AU)
Interstitial fibrosis area (%)
Sh
Nx

Figure 4

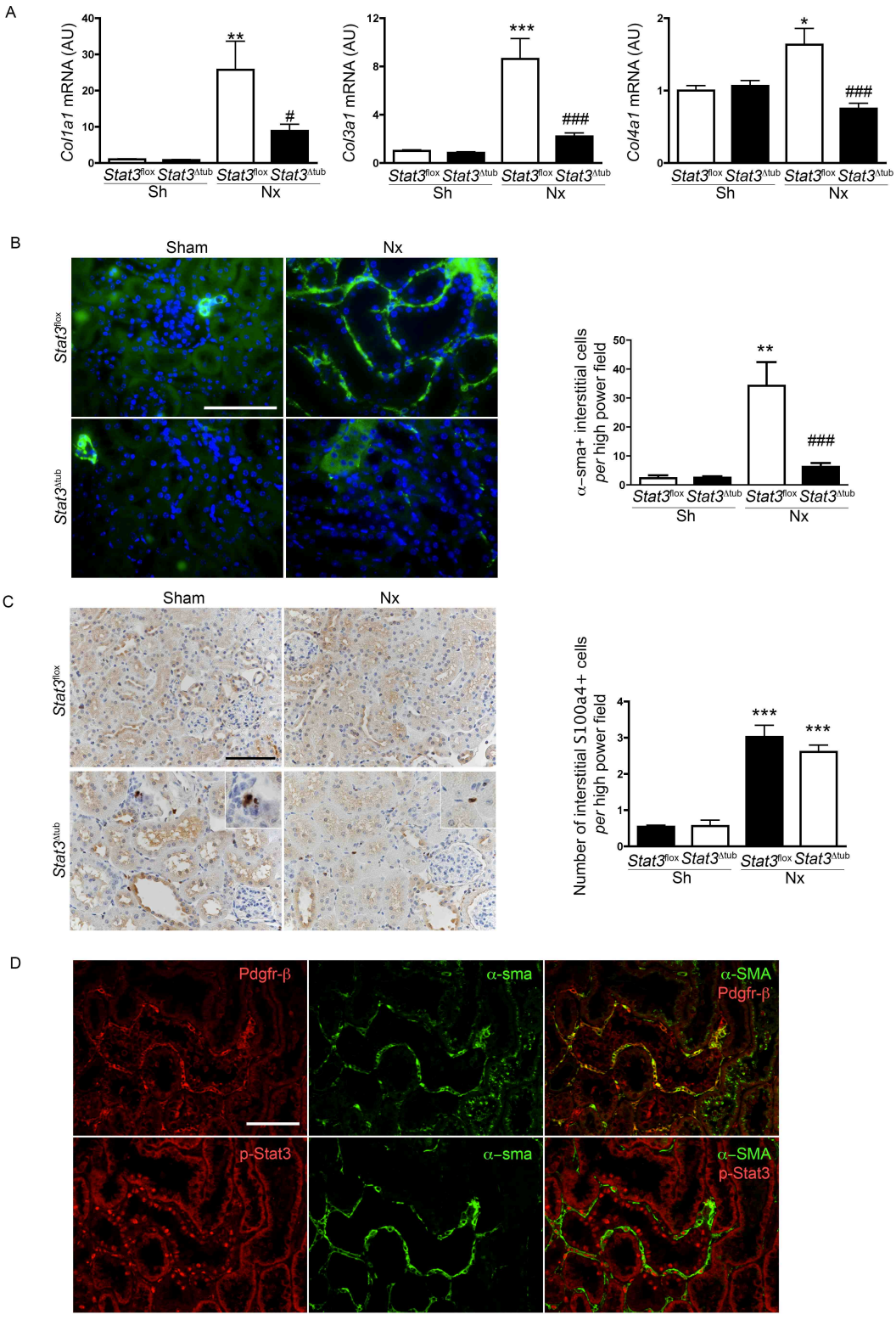
A
Col1a1 mRNA (AU)
Col3a1 mRNA (AU)
Col4a1 mRNA (AU)
Stat3flox Stat3Δtub Stat3flox Stat3Δtub
Sh
Nx
B
Sham
Nx
Stat3flox
Stat3Δtub
α–sma+ interstitial cells per high power field
C
Number of interstitial S100a4+ cells per high power field
D
Pdgfr-β
α-sma
α-SMA Pdgfr-β
p-Stat3
α–sma
α–SMA p-Stat3

Figure 5

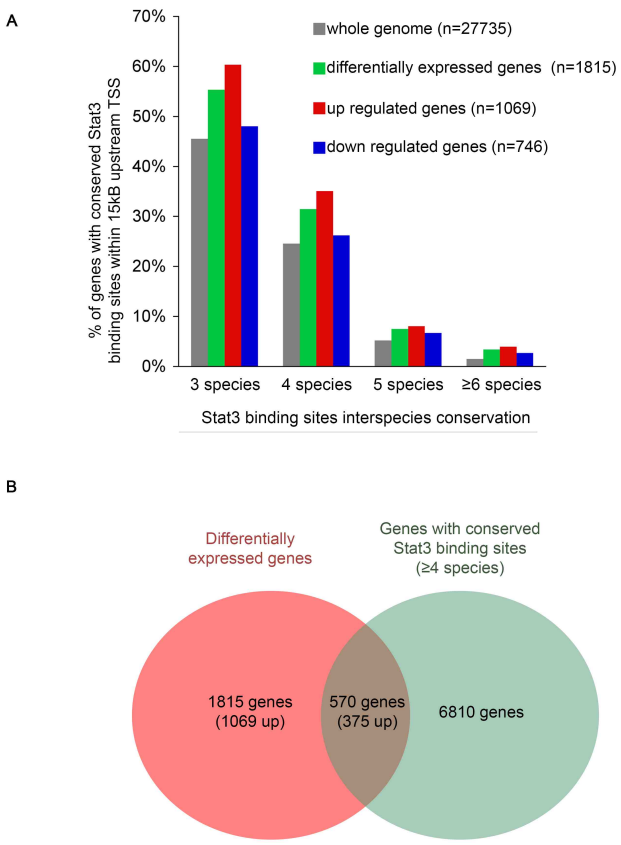
A
70%
60%
50%
40%
30%
20%
10%
0%
% of genes with conserved Stat3 binding sites within 15kB upstream TSS
whole genome (n=27735)
differentially expressed genes (n=1815)
up regulated genes (n=1069)
down regulated genes (n=746)
3 species
4 species
5 species
≥6 species
Stat3 binding sites interspecies conservation
B
Differentially expressed genes
Genes with conserved Stat3 binding sites (≥4 species)
1815 genes (1069 up)
570 genes (375 up)
6810 genes

Figure 6

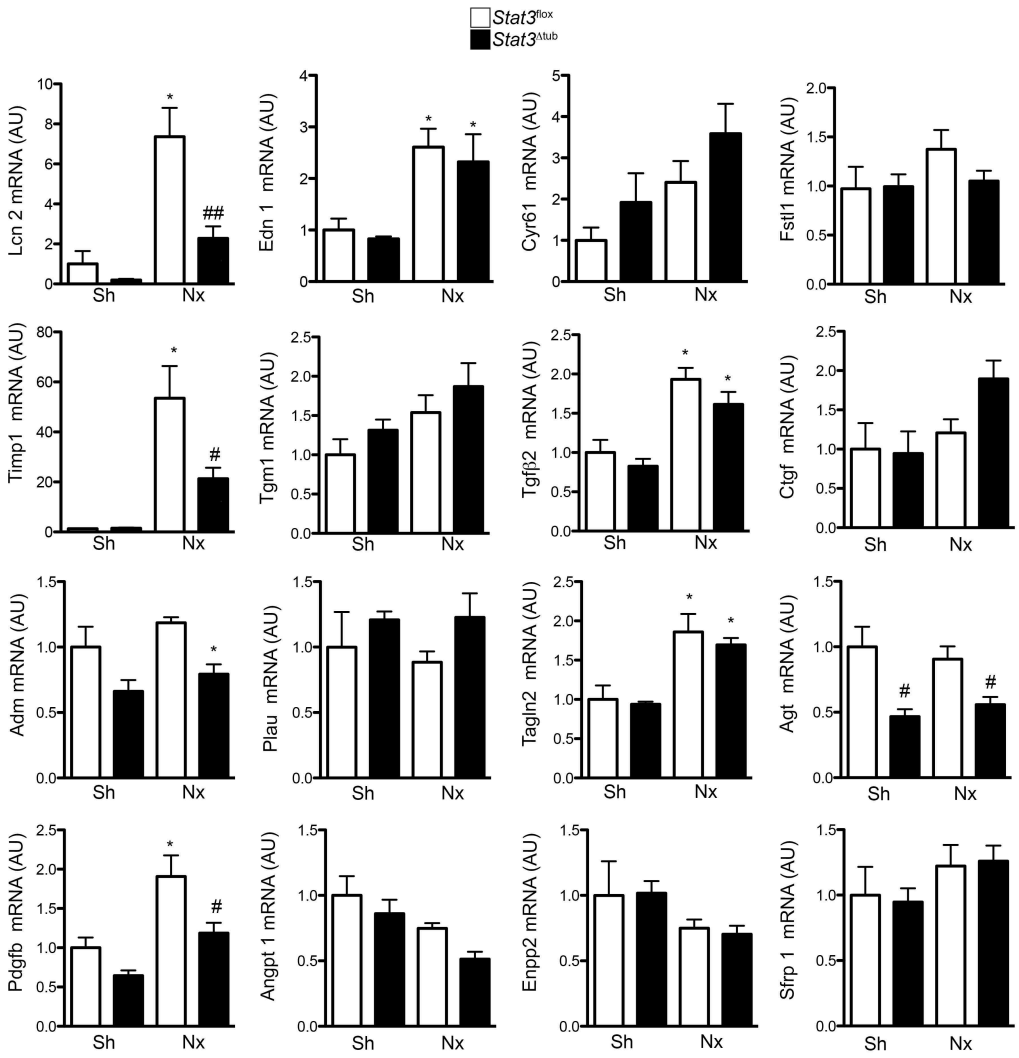
Stat3flox
Stat3Δtub
Lcn 2 mRNA (AU)
Edn 1 mRNA (AU)
Cyr61 mRNA (AU)
Fstl1 mRNA (AU)
Timp1 mRNA (AU)
Tgm1 mRNA (AU)
Tgfβ2 mRNA (AU)
Ctgf mRNA (AU)
Adm mRNA (AU)
Plau mRNA (AU)
Tagln2 mRNA (AU)
Agt mRNA (AU)
Pdgfb mRNA (AU)
Angpt 1 mRNA (AU)
Enpp2 mRNA (AU)
Sfrp 1 mRNA (AU)
Sh
Nx

Figure 7

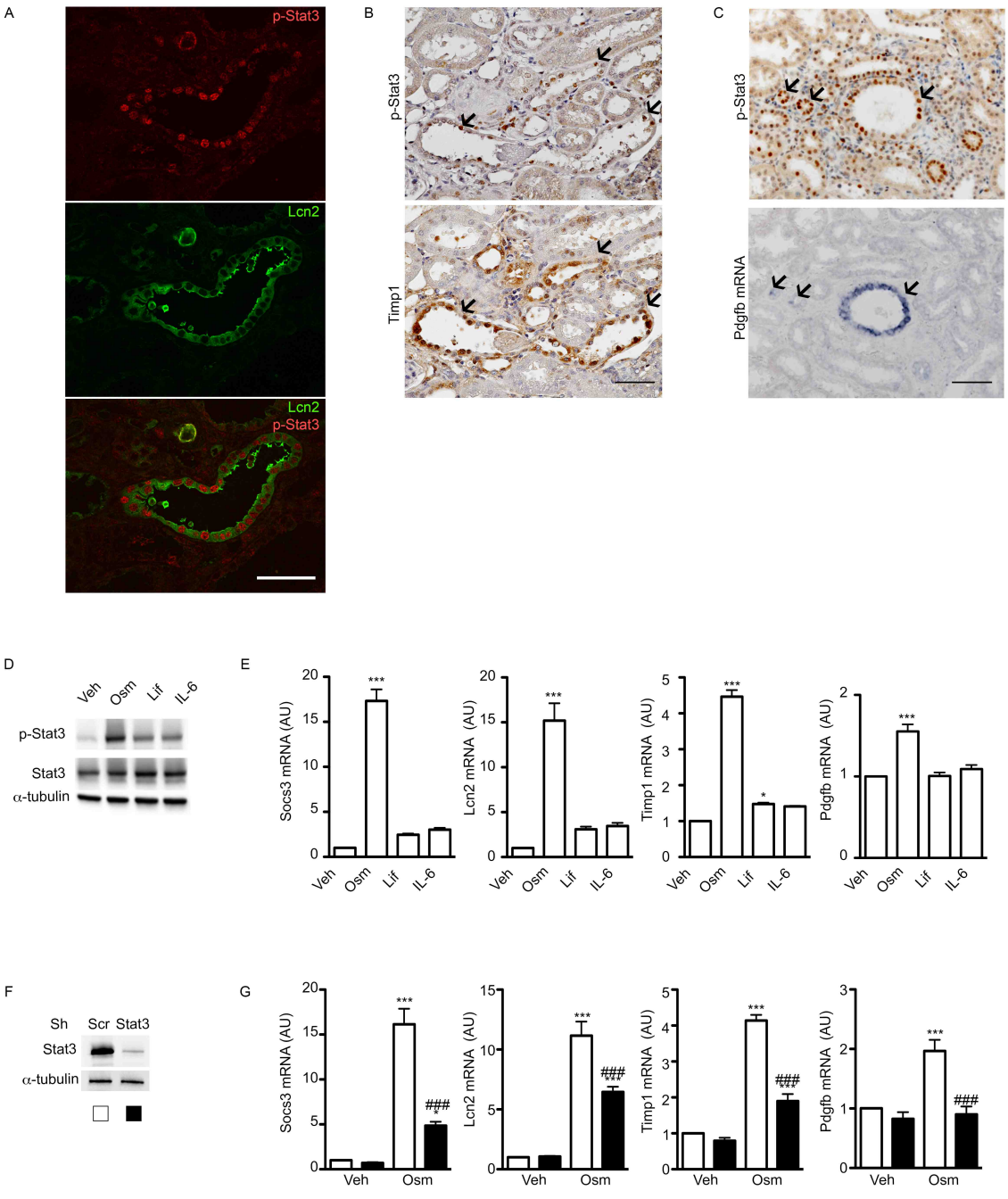
A
p-Stat3
Lcn2
Lcn2
p-Stat3
B
p-Stat3
Timp1
C
p-Stat3
Pdgfb mRNA
D
Veh
Osm
Lif
IL-6
p-Stat3
Stat3
α-tubulin
E
Socs3 mRNA (AU)
Lcn2 mRNA (AU)
Timp1 mRNA (AU)
Pdgfb mRNA (AU)
Veh
Osm
Lif
IL-6
F
Sh
Scr
Stat3
Stat3
α-tubulin
G
Socs3 mRNA (AU)
Lcn2 mRNA (AU)
Timp1 mRNA (AU)
Pdgfb mRNA (AU)
Veh
Osm

Figure 8

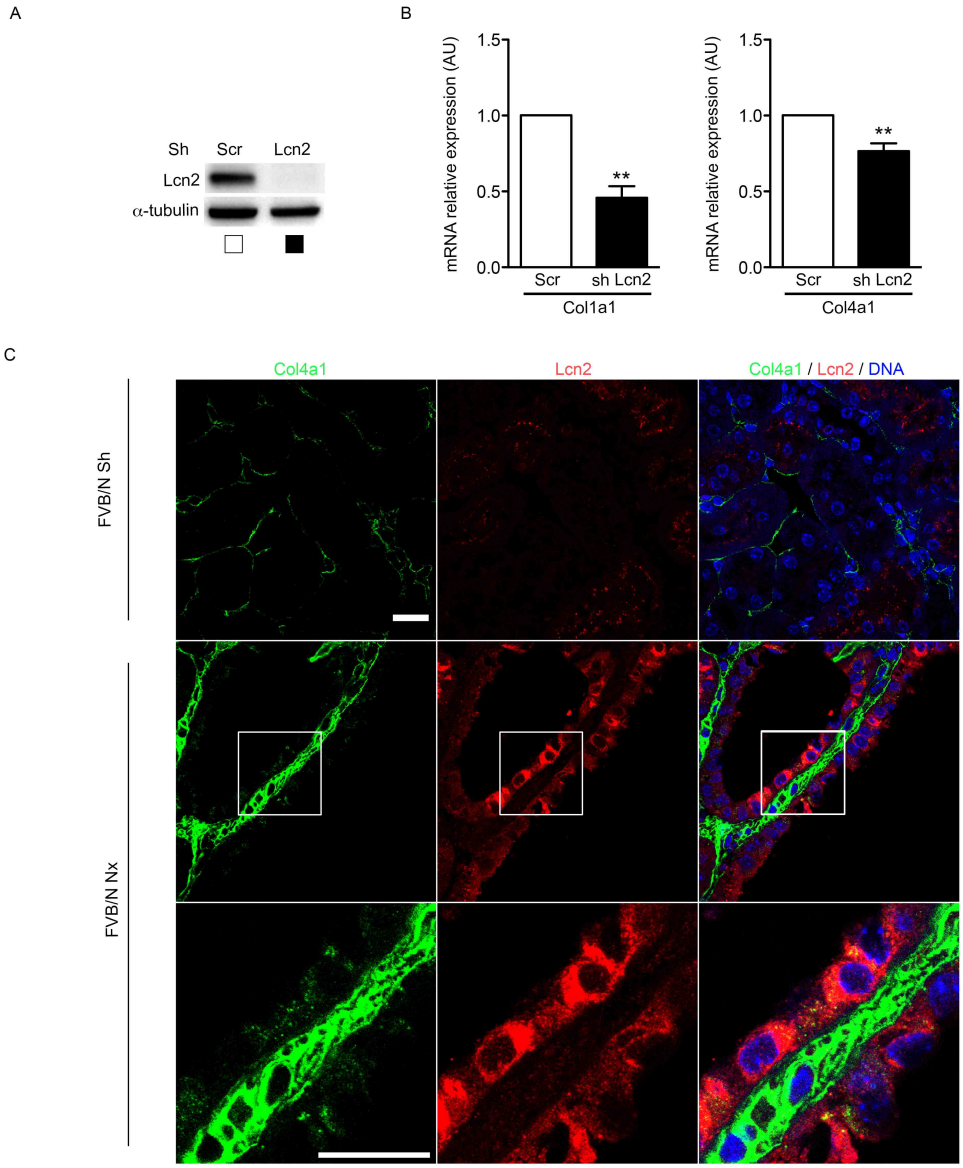
A
Sh
Scr
Lcn2
Lcn2
α-tubulin
B
mRNA relative expression (AU)
1.5
1.0
0.5
0.0
**
Scr
sh Lcn2
Col1a1
mRNA relative expression (AU)
1.5
1.0
0.5
0.0
**
Scr
sh Lcn2
Col4a1
C
Col4a1
Lcn2
Col4a1 / Lcn2 / DNA
FVB/N Sh
FVB/N Nx

Figure 9